3D trapping and manipulation of micro-particles using holographic optical tweezers with optimized computer-generated holograms

Tao Tao (陶　陶)[1], Jing Li (李　静)[1*], Qian Long (龙　潜)[1], and Xiaoping Wu (伍小平)[2]

[1]*Department of Precision Machinery and Precision Instrumentation, University of Science and Technology of China, Hefei 230027, China*

[2]*Department of Modern Mechanics, University of Science and Technology of China, Hefei 230027, China*

Corresponding author: lijing@ustc.edu.cn

A multi-plane adaptive-additive algorithm is developed for optimizing computer-generated holograms for the reconstruction of traps in three-dimensional (3D) spaces. This algorithm overcomes the converging stagnation problem of the traditional multi-plane Gerchberg–Saxton algorithm and improves the diffraction efficiency of the holograms effectively. The optimized holograms are applied in a holographic optical tweezers (HOT) platform. Additionally, a computer program is developed and integrated into the HOT platform for the purpose of achieving the interactive control of traps. Experiments demonstrate that the manipulation of micro-particles into the 3D structure with optimized holograms can be carried out effectively on the HOT platform.

OCIS codes: 090.1760, 350.4855.

doi: 10.3788/COL201109.120010.

Since its invention by Ashkin[1], optical tweezers have been applied in several branches of the physical and life sciences, such as in manipulating cells, sorting particles[2], trapping nano-particles, and so on. In many applications, such as photonic-crystal construction, the creation of metrological standards within nanotechnology and the seeding of tissue growth[3], the ability of three-dimensional (3D) trapping and manipulation of micro-particles is required. Holographic optical tweezers (HOT) use a phase-only spatial light modulator (SLM) to dynamically display computer generated holograms (CGHs)[4] that can create complicated 3D configurations of traps simultaneously.

In order to reconstruct the desired 3D trapping patterns, computer hologram algorithm is important. Several phase retrieval algorithms used for designing CGHs have been reported, such as gratings and lenses[5], quadrant kinoform[6], and multi-plane Gerchberg-Saxton (GS)[7]. The multi-plane GS algorithm has been applied in most holographic optical tweezer systems due to a combination of calculation speed and reconstruction quality. However, the multi-plane GS algorithm inherits the converging stagnation problem from the GS algorithm, which could lead to stagnation in a local optimum. In this letter, we extend the adaptive-additive (AA)[8] algorithm into 3D case to optimize the computer-generated phase holograms for the formation of multiple traps in arbitrary 3D positions. We also demonstrate the improvement and compare it with the conventional multi-plane GS algorithm. The optimized computer-generated holograms are performed on a SLM-based HOT platform, which includes an integrated MATLAB program used for driving the SLM and providing a user interface that allows users to interactively control the traps. Experiments of dynamic 3D trapping and manipulation of micro-particles on the platform are also conducted.

In a two-dimensional (2D) situation, the AA algorithm can solve the converging stagnation problem of the GS algorithm and enhance the quality of the reconstructed image without a significant increase in computation time[9]. In this letter, we design a multi-plane AA algorithm for optimizing computer-generated holograms in the reconstruction of trap arrays in an arbitrary 3D pattern.

As a multi-plane GS algorithm, the AA algorithm belongs to the group of iterative Fourier transformation algorithms (IFTAs). This algorithm takes advantage of the fact that there is a Fourier transform relationship between the complex fields at the hologram plane and the focal plane of the objective lens, and that such relationship can be shifted to any out-of-focus output plane in the image space of the objective lens by introducing a holographic lens.

As shown in Fig. 1, the holographic lens changes the focal length of the entire system, thereby resulting in an axial displacement. The phase distribution necessary to accomplish this movement is defined by

$$\phi_{\text{lens},d} = \frac{2\pi d}{\lambda df^2}(x_{\text{h}}^2 + y_{\text{h}}^2), \qquad (1)$$

where f is the focal length, df is the distance from the output plane to the focal plane of the objective lens, and λ is the wavelength. Considering a phase hologram with phrase profile ϕ_{h} displayed on the SLM and illuminated by a laser beam with amplitude A_{in}, the complex field $E_{\text{out},d}$ on the output plane can be calculated by

$$E_{\text{out},d} = \mathscr{F}\{A_{\text{in}}\exp[\text{i}(\phi_{\text{h}} - \phi_{\text{len},d})]\}. \qquad (2)$$

For reconstructing multiple traps in 3D space, multiple 2D planes at different depths corresponding with trap positions were chosen as a set of output planes. In Fig. 2,
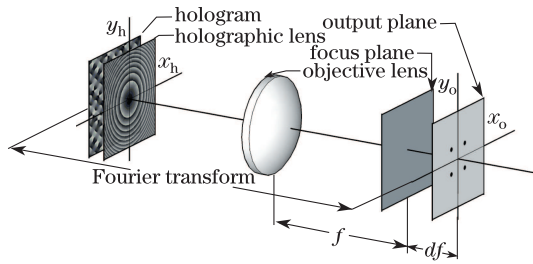
Fig. 1. Reconstructions at an out-of-focus output plane. The focus plane of the objective lens can be shifted by introducing a holographic lens.
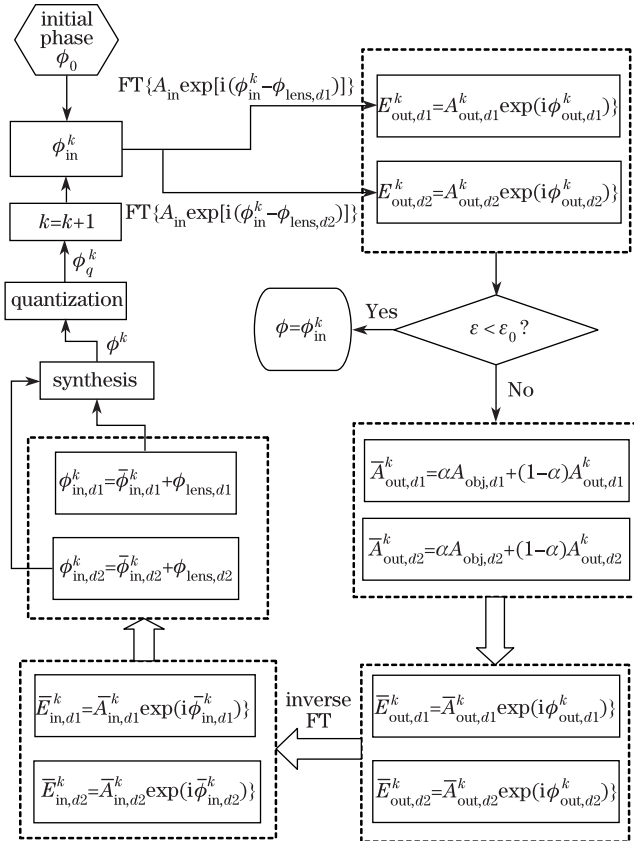

Fig. 2. Example of two planes with the multi-plane AA algorithm.

we depict the flowchart of the multi-plane AA algorithm with two output planes at different axial positions ($d1$ and $d2$). At the beginning of the kth iteration, the phase distribution of the hologram is ϕ_{in}^k. The complex amplitudes at each output plane ($E_{\text{out},d1}^k$, $E_{\text{out},d2}^k$) can be calculated through Eq. 2. The deviations between the calculated amplitude fields ($A_{\text{out},d1}^k$, $A_{\text{out},d2}^k$) and the desired amplitude fields ($A_{\text{obj},d1}$, $A_{\text{obj},d2}$) can be computed by an error function ε given by

$$\varepsilon = \sum_i \sum_{x,y} \left(A_{\text{out},i}^k - A_{\text{obj},i} \right)^2, \tag{3}$$

where $i = d1, d2$. If the value of ε is higher than an acceptable tolerance ε_0, the intensity constraints are computed by mixing a proportion of the desired amplitudes into the calculated fields as

$$\overline{A}_{\text{out},i}^k = \alpha A_{\text{obj},i} + (1 - \alpha) A_{\text{out},i}^k, \tag{4}$$

where $i = d1$, $d2$ and α is a coefficient to be chosen.

We kept the phases of the result fields but replaced the amplitudes with the intensity constraints to obtain new complex fields ($\overline{E}_{\text{out},d1}^k$, $\overline{E}_{\text{out},d2}^k$). Afterwards, we backward propagated the new fields through inverse Fourier transform. The amplitudes of $\overline{E}_{\text{in},d1}^k$, $\overline{E}_{\text{in},d2}^k$ were abandoned, because we wanted to optimize for a phase-only hologram. The phases of holographic lenses ($\phi_{\text{lens},d1}$, $\phi_{\text{lens},d2}$) were added back on purpose to generate the defocus value of each output plane. Finally, the retrieved phase fields ($\phi_{\text{in},d1}^k$, $\phi_{\text{in},d2}^k$) in one iteration loop were synthesized, and then quantized in accordance with the phase levels of the SLM. The synthesis of phase holograms for each plane is described by

$$\phi^k = \text{mod}(\sum_i \phi_{\text{in},i}^k, 2\pi), \quad i = d1, d2, \tag{5}$$

where $i = d1, d2$. The final obtained phase hologram ϕ_k was used as the starting point of the subsequent iteration. The cycle was repeated until the difference between the calculated and desired fields became non-significant. As a measure for optimization quality, it is possible to utilize the diffraction efficiency of the hologram and the uniformity of trap pattern. For the diffraction efficiency η, we use the following definition:

$$\eta = \sum_{k=1}^n I_k \Big/ I_{\text{total}}, \tag{6}$$

where n is the number of traps, and $I_k = |E_{\text{out}}(x_k, y_k, z_k)|^2$ is the light intensity at desired position of the kth trap. In addition, I_{total} represents the total power of the incident beam and can be calculated at the hologram plane using

$$I_{\text{total}} = MN \sum_{i=1}^M \sum_{j=1}^N A_{\text{in}}^2(x_i, y_j), \tag{7}$$

where $M \times N$ is the total number of pixels in the hologram. The standard deviation of trap intensity σ describing the uniformity error is defined as

$$\sigma = \sqrt{\sum_{k=1}^n \left[\frac{I_k - \overline{I}}{\overline{I}} \right]^2 \Big/ n - 1}, \tag{8}$$

where $\overline{I} = \sum_{k=1}^n I_k/n$ is the average intensity of traps.

With the multi-plane AA algorithm, a CGH for a 3D trap pattern, consisting of 8 traps with uniform intensity in 2 planes at distances $df = \pm 5~\mu$m was optimized. Figure 3 shows the intensity images at 2 planes with 512×512 pixels, with each spot representing a trap with 1×1 pixel.

Typically, the 2D AA algorithm requires 8 or more iterations to converge. In this letter, the iteration loop is repeated 50 times to ensure that the algorithm converged; in addition, an intermediate value for the adaptive coefficient, α=0.6, is used. The focal length with a commercial high numerical aperture microscope objective lens of f=2 mm is adopted, and a random phase profile is chosen as ϕ_0. With the aim of improving the
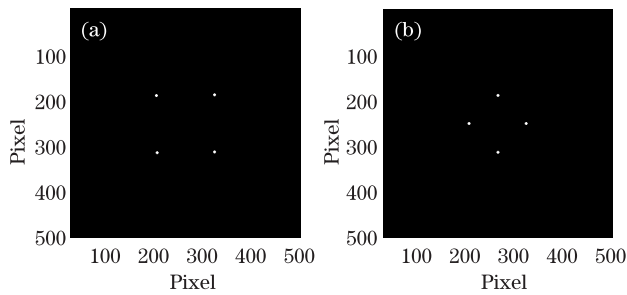
Fig. 3. Desired intensity images at two output planes. (a) $df=-5$ μm and (b) $df=+5$ μm.
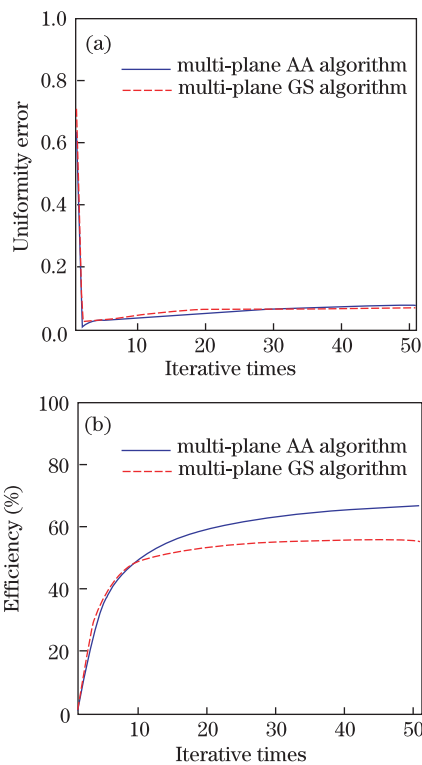

Fig. 4. Evolutions of (a) uniformity error σ and (b) diffraction efficiency η.

algorithm performance, additional phase hologram is computed using standard multi-plane GS algorithm with same parameters and initial phase. The two algorithms are both implemented in MATLAB. Each iteration of the multi-plane AA algorithm took about 200 ms on a Core i5-2800 CPU, which is almost the same as the multi-plane GS algorithm.

The evolutions of the uniformity error σ and the diffraction efficiency η during iterations with multi-plane GS algorithm and multi-plane AA algorithm are shown in Fig. 4, and their respective values after 10, 20, 30, 40, and 50 iterations are listed in Table 1.

The uniformity errors of both algorithms decrease rapidly in several initial iterations. During subsequent iterations, the values of the two algorithms slightly increase by almost the same amount and are maintained at an acceptable low level. This effect may be caused by increasing the energy of traps in iterations. The diffraction efficiency curves show the superiority of the multi-plane AA algorithm. In the first 10 iterations, the multi-plane AA algorithm converges at the same speed as that

recorded in the multi-plane GS algorithm. In the following iterations, as the stagnation effect of multi-plane GS algorithm is observed, the diffraction efficiency of multi-plane AA algorithm continues to increase, reaching 66.8% after 50 iterations, which is approximately 11.2% higher than that of the multi-plane GS algorithm.

The scheme of the HOT system is shown in Fig. 5. A linearly polarized laser beam was expanded and collimated by a beam expander. Before illuminating the phase-only SLM, the polarization direction and incident angle of the beam were adjusted by a half wave plate; mirrors M1 and M2 were also used to meet the conditions assumed by the manufacturer. The purpose of the SLM was to modify the phase of the incoming beam wave front. A telescope was adopted to reduce the size of the modified beam to fill the entrance pupil of a microscope objective and image the SLM onto the pupil plane. After passing through the telescope, the beam was reflected by a dichroic mirror, which was used to separate the laser

Table 1. Results of the Simulation of Multi-plane AA and Multi-plane GS Algorithms

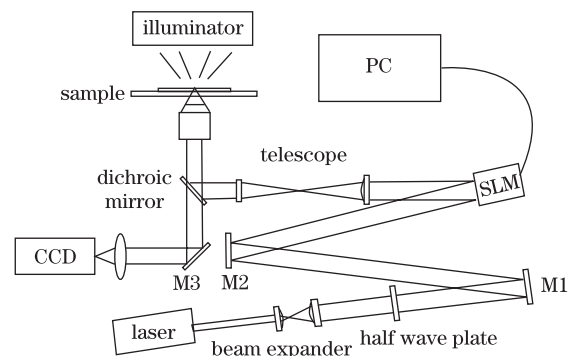| Iterative Times	10	20	30	40	50
σ(multi-plane AA)	0.0345	0.0535	0.0667	0.0743	0.0780
η(multi-plane AA)	51.4%	60.0%	64.0%	66.0%	66.8%
σ(multi-plane GS)	0.0488	0.0632	0.0671	0.0704	0.0716
η(multi-plane GS)	49.9%	54%	55.3%	55.7%	55.6%

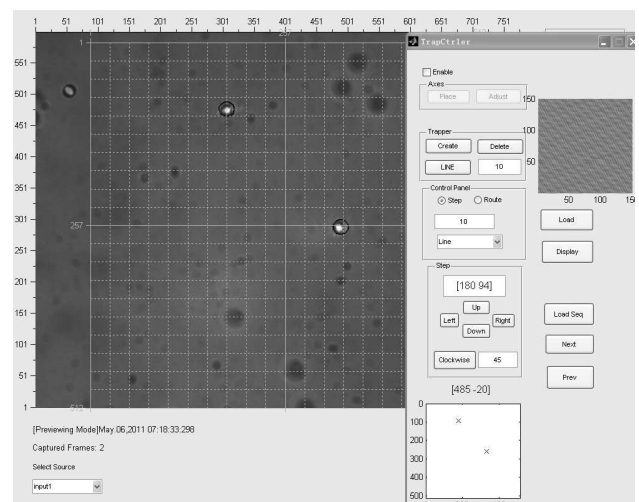Fig. 5. Schematic diagram of a holographic optical tweezers system.

Fig. 6. User interface for the software.
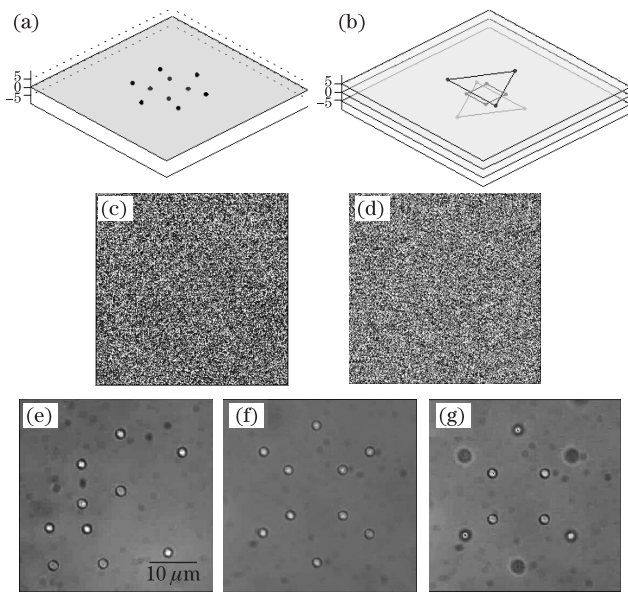
Fig. 7. Arrangement of trapped 2.5 μm polystyrene spheres into the 3D structure. (a) 2D targeted pattern, (b) 3D targeted structure, (c) phase holograms for the 2D targeted traps pattern, and (d) the 3D targeted structure. The captured photos of (e) the initial distribution of polystyrenes, (f) 2D array of polystyrenes, and (g) the 3D distribution of polystyrenes.

beam and light of illuminator, and then focused on the sample plane by the high numerical aperture microscope objective. A CCD camera recorded the experiments.

A MATLAB program that can be integrated into the HOT system described above has been developed. The program allows user to interactively control the traps with a user interface, as shown in Fig. 6. In this program, a live video acquired with CCD camera is displayed as background of the window to show the real-time status of the micro-particles. The grid indicates the area of trapping plane, which is limited by the spatial resolution of the SLM. Circles overlaid on the video provide a visual feedback on the positions of the optical traps and can be added, moved, and deleted individually with the computer mouse. An additional dialog box is displayed to show the pattern consisting of traps, coordinates of each trap, and the CGH displayed on the SLM currently. It also provides some useful operations, such as loading a sequence of CGHs, creating traps in specific configuration, and assigning routes of movements of optical traps. With existing hologram design algorithms, such as GS algorithm, the program can realize real-time control of optical traps in 2D plane. In addition, 3D traps control can be carried out by playing a sequence of CGHs pre-calculated with the multi-plane AA algorithm.

Our HOT platform was built on a Boulder Nonlinear Systems PM512 SLM capable of providing phase-only

modulation over a range of [0, 2π] radians. A Nd:YAG solid state laser with 1-W power operating at 532 nm was used as light source. The laser beam was tightly focused with a 100$\times$NA1.25 Nikon oil immersion microscope objective. Figure 7 demonstrates an example of 3D trapping and manipulation of micro-particles in the water. Two stages were adopted to fulfill the experiment. First, 10 polystyrene spheres with a diameter of 2.5 μm were interactively trapped and moved in the focus plane to form a 2D pattern from the arbitrary initial positions, as shown in Fig. 7(a). Then, a sequence of pre-calculated CGHs was designed based on the multi-plane AA algorithm and displayed on SLM, which changed the trap array from the 2D pattern into the 3D configuration (Fig. 7(b)) with 10 intermediate steps. The trapping planes were separated at a maximal distance of 10 μm along the axial direction. Figures 7(f) and (g) show the photos of spheres trapped in 2D and 3D configurations, respectively. The corresponding CGHs are displayed in Figs. 7(c) and (d).

In conclusion, because of its high efficiency, a multiplane AA algorithm is developed and used to compute GCHs for generating traps in 3D space. A holographic optical tweezers system is set up with an integrated MATLAB program that provides an effective approach to control the positions of traps. Experiments demonstrate that our hologram design algorithm and HOT platform can arrange micro-particles into complex 3D structures from an arbitrary initial position and can be applied in the fabrication of micro-nano devices.

References

1. A. Ashkin, J. M. Dziedzic, J. E. Bjorkholm, and S. Chu, Opt. Lett. **11,** 288 (1986).
2. D. G. Grier, Nature **424,** 810(2003).
3. J. Leach, G. Sinclair, P. Jordan, J. Courtial, M. J. Padgett, J. Cooper, and Z. J. Laczik, Opt. Express **12,** 220 (2004)
4. G. Wang, C.Wen, and A. Ye, J. Opt. A **8,** 703 (2006).
5. J. Liesener, M. Reicherter, T. Haist, and H. J. Tiziani, Opt. Commun. **185,** 7782 (2000).
6. F. Belloni and S. Monneret, Appl. Opt. **46,** 4587 (2007).
7. G. Sinclair, J. Leach, P. Jordan, G. Gibson, E. Yao, Z. Laczik, M. Padgett, and J. Courtial, Opt. Express **12,** 1665 (2004).
8. E. R. Dufresne, G. C. Spalding, M. T. Dearing, S. A. Sheets, and D. G. Grier, Rev. Sci. Instrum. **72,** 1810 (2001).
9. J. Bu, G. Yuan, Y. Sun, S. Zhu, and X. Yuan, Chin. Opt. Lett. **9,** 061202 (2011).